Eur. Phys. J. B **41**, 479–483 (2004)
DOI: 10.1140/epjb/e2004-00341-4

THE EUROPEAN PHYSICAL JOURNAL B

Formation of silver particles and silver oxide plume nanocomposites upon pulsed-laser induced liquid-solid interface reaction

Q.X. Liu[1,2], C.X. Wang[1], and G.W. Yang[1,a]

[1] State Key Laboratory of Optoelectronic Materials and Technologies, School of Physics and Engineering, Zhongshan University, Guangzhou 510275, P.R. China
[2] Department of Applied Physics, Guangdong University of Technology, Guangzhou 510090, P.R. China

Received 6 April 2004
Published online 5 November 2004 –

Abstract. Nanodendrites consisting of silver and silver oxide are grown upon a pulsed-laser induced reaction at the interface between the solid target and silver nitrate solution. By using a high-resolution transmission electron microscope (HRTEM) equipped with an energy dispersive X-ray spectrometer (EDS) and selected area diffraction (SAD), the fabricated nanopatterns are identified to be a composite structure that consisting of silver nanoparticles and silver oxide nanoplumes with polycrystalline structure. In detail, these silver nanocrystals are trunks of the nanodendrite, and their size is in the range of 30 to 50 nm. The silver oxide nanoplumes are branches of the nanodendrite, and their width and length are in the ranges of 20 to 50 nm and 30 to 100 nm, respectively. Additionally, we suggested a vapor-liquid mechanism for the formation of the nanopatterns using a pulsed-laser induced liquid-solid interface reaction, in which both silver clusters in vapor and silver ions in solution are simultaneously involved.

PACS. 81.15.Fg Laser deposition – 61.46.+w Nanoscale materials: clusters, nanoparticles, nanotubes, and nanocrystals – 81.07.Bc Nanocrystalline materials

1 Introduction

Metal and metallic oxide nanoparticles play important roles in many different areas, such as photography, biological labeling, photonics, optoelectronics, information storage, and formulation of magnetic ferrofluids [1–3]. Basically, the intrinsic properties of a metal and metallic oxide nanoparticle are mainly determined by their size, shape, composition, and crystalline structure. Therefore, in principle, one can control any one of these parameters to fine-tune the properties of this nanoparticle. It is well known that silver and its oxide have important applications in photography, micro-electronic, catalysis, and battery industries. The nanoparticle synthesis of silver and its oxide has thus received considerable attention in recent years [4]. Traditional methods producing nanoparticles include mechanical milling, spray pyrolysis, chemical precipitation, and vapor deposition. In turn, each of these techniques have advantages and disadvantages [5,6]. Recently, we developed a novel pulsed-laser induced liquid-solid interfacial reaction (PLIIR) to synthesize metastable nanoparticles [7]. Interestingly, a series of diamond and related materials nanocrystals has been prepared by PLIIR [8–12]. Note that two points can be deduced from PLIIR investigations [13], one point is that PLIIR is likely to synthesize metastable nanocrystals, and another is that the new phase formation involves both liquid and solid. In this paper, we report an abnormal nanodendrite growth of silver and silver oxide upon a pulsed-laser induced reaction in the silver nitrate solution. To the best of our knowledge, few studies concerning the nanodendrite formation of silver and its oxide have been reported in the literature.

2 Experimental

The preparation system was described in detail in reference [7]. Briefly, the second harmonic is produced by a Q-switch Nd:YAG laser with a wavelength of $\lambda = 532$ nm, a pulse width of $\tau = 10$ ns, a repeating frequency of $\nu = 3$ Hz, and a power density of $p = 10^7$ W/cm^2. In our experiment, the saturated silver nitrate solution with chemical purity of 99.999% is used as the reactive liquid, and the solid target is a single nickel bulk with a purity of 99.99%. The nickel target was first fixed on the bottom of a reactive chamber, and then the silver nitrate solution was poured slowly into the chamber until the target was covered by 1−2 mm. Finally, the pulsed-laser was focused onto the target surface. During the laser ablation,

[a] e-mail: stsygw@zsu.edu.cn

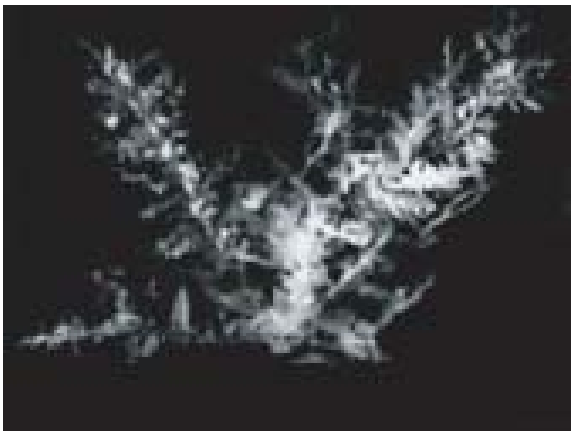

Fig. 1. SEM micrograph of the dendrites grown by pulsed-laser ablation in silver nitrate solution.

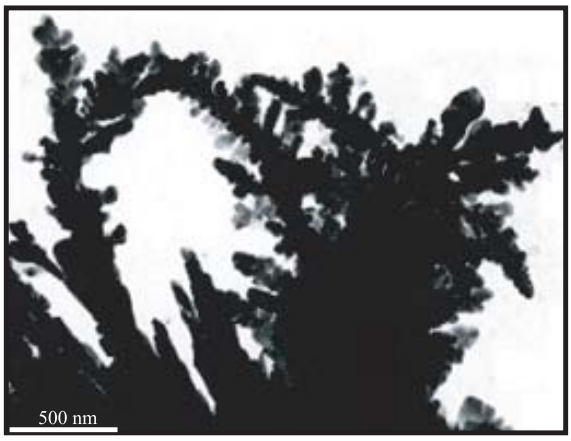

(a)

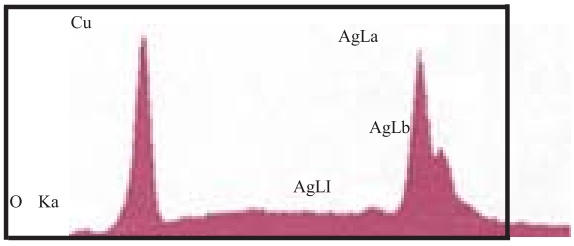

(b)

Fig. 2. TEM bright field image (a) of the fractal-like nanodendrites grown upon pulsed-laser irradiation in a silver nitrate solution, and the corresponding EDS analysis (b).

the target and solution were maintained at room temperature, and the target was rotated at the slow speed (20 rotations per minute). After the laser interacting with the target for more than 120 minutes, the powders were collected from the surface of the solution. The synthesized powders were analyzed. It is found that PLIIR is a flexible method to fabricate nanostructures [9–11]. The laser parameters, such as laser power and repeating frequency, can greatly affect the structure and composition of the productions [13,14]. Scanning electron microscope (SEM), HRTEM (JEM-2010, 200kV) equipped with EDS within the measuring error of 2 at % and SAD are employed to identify the morphology, composition, and crystalline structure of the synthesized samples by PLIIR. Cu grids are employed to hold the samples.

3 Results and discussions

Figure 1 shows the SEM image of the synthesized products through pulsed-laser ablation at the interface between the nickel target and silver nitrate solution. Obviously, we can see that the grown pattern displays the shape of a tree that should belong to the dendrite growth. Meanwhile, the typical fractal-like pattern is evidenced by the bright field image from the TEM shown in Figure 2a. Similarly, one can see that the tree-shaped nanodendrites are fabricated by a pulsed-laser induced reaction in the silver nitrate solution. Furthermore, the corresponding EDS analysis of Figure 2a is shown in Figure 2b. The compositions of the grown nanodendrites are found to be silver and oxygen from Figure 2b, and the percentage of silver in the pattern is about 90%. It is shown that quite strong peak from Cu arises from the Cu grids employed to hold the samples in Figure 2b. The bright field images from the TEM show detailed structures of the synthesized nanodendrites, as shown in Figure 3. Interestingly, one can see from Figures 3a and b that these nanodendrites mainly consist of trunks and branches. The trunks are stacked by the nanoparticles with perfect crystalline faces, which are silver nanoparticles according to the corresponding EDS analysis (see the inset in Fig. 3a). The average size of these nanoparticles is about 50 nm. Meanwhile, the branches display plume-like (nanoplume) features, growing radially from the trunks. Silver and oxygen compositions in the nanoplumes are then determined by the corresponding EDS analysis (see the inset in Fig. 3b). The width and length of these nanoplumes are in the ranges of 20 to 50 nm and 30 to 100 nm, respectively. For determining crystalline structures of the nanodendrites, the corresponding SAD pattern of Figure 3 is shown in Figure 4. Based on the SAD analysis, the crystalline structures of the grown nanodendrites are identified to be a polycrystalline structure, including a mixture of face center cubic (fcc) silver and orthorhombic silver oxide (Ag_2O_3) from Figure 4. In other words, these nanodendrites indeed consist of Ag nanoparticles and Ag_2O_3 nanoplumes (Figs. 2, 3, and 4). Tables 1 and 2 list the results of the Ag and Ag_2O_3 crystalline structures, respectively. The error in the lattice parameters determined by SAD is less than 4%. Accordingly, these results show that the abnormal nanodendrites consisting of silver nanoparticles and silver oxide nanoplumes are grown upon a pulsed-laser induced reaction in the silver nitrate solution. Note that simple silver, nickel, and their oxide nanoparticles are also encountered in the products. Silver and nickel are immiscible from the point of view of equilibrium thermodynamics. Normally, silver could therefore not form an alloy phase with nickel by conventional techniques, due to the

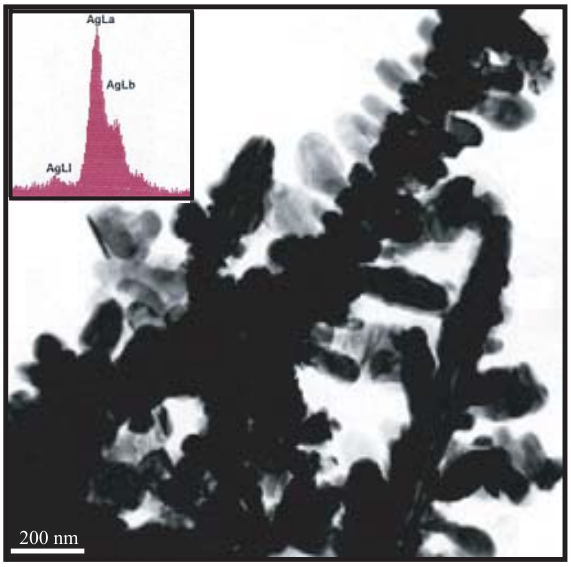

(a)

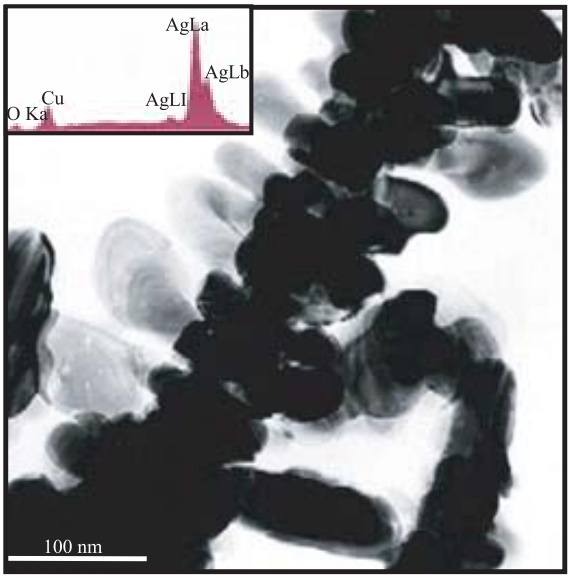

(b)

Fig. 3. TEM bright field image (a) and (b) of the detail structures of the silver nanoparticles and silver oxide nanoplumes, two insets in (a) and (b) are the corresponding EDS analysis for silver and silver oxides, respectively.

repulsive interaction between Ag and Ni atom [15]. Therefore, with a pulsed-laser power density of $p = 10^7$ W/cm^2, apart from nickel nanoparticles, we did not find the silver and nickel alloy phase. However, the silver and nickel alloy phase can be detected in the products from PLIIR when the pulsed-laser power density was increased to 10^{10} W/cm^2 [14]. Accordingly, the laser parameters such as laser power can greatly affect the structure and composition of the productions from PLIIR. Moreover, the percentages of these nanocrystals are less than 40% according to our TEM statistics. A majority of the nanostructures in

Fig. 4. The corresponding SAD pattern of the grown nanodendrites, and two polycrystalline structures can be identified for fcc silver and orthorhombic silver oxides, respectively.

the products are the stable Ag and Ag_2O_3 nanodendrites. These results therefore indicate that both nanocrystals and nanoplumes are easily synthesized by pulsed-laser induced reaction in the silver nitrate solution. Then, compared with other nanoparticles, the nanodendrites formation seems preferable.

Now, we turn to discuss the formation of the silver and silver oxide nanodendrites upon a pulsed-laser induced reaction in the silver nitrate solution. PLIIR is a relatively new laser-based materials synthesis, and has received considerable attention in recent years [16–21]. According to our previous studies [9–11] and Poondi and Singh's studies [16,17], we proposed a vapor-liquid mechanism of the nanostructure formation upon PLIIR, in which both silver clusters in vapor and silver ions in solution are simultaneously involved. Three distinct sequential stages are suggested to generate Ag and Ag_2O_3 nanodendrites. The first stage is a pre-nucleation process. The substrate is heated by absorbing the energy from the laser pulse when the pulsed-laser irradiates the surface of the substrate. The thermal energy from the laser pulse could facilitate the production of metal atoms from the solution and the substrate by chemical reduction, pyrolytic, or ionic processes [17]. Meanwhile, a plasma plume with high- pressure and high-temperature (HPHT) is generated at the interface between the substrate and the solution. The plasma plume is a mixture of silver, nickel, oxygen, and their ions. The second stage is a nucleation and growth process. The intense thermal diffusion of the species in the

Table 1. Identification of the orthorhombic phase silver oxide grown upon pulsed-laser induced in silver nitrate solution. D_{exp} are the experimental data, D_{calc} are the calculated values.

(*hkl*)	D_{exp} (Å)	D_{calc} (Å)
(120)	4.86	4.86
(220)	4.06	4.07
(101)	3.45	3.47
(231)	2.69	2.69
(311)	2.46	2.48
(411)	2.38	2.36
(520)	2.28	2.31
(331)	2.18	2.18
(511)	2.08	2.07
(440)	2.05	2.03
(620)	1.94	1.98
(151)	1.81	1.80
(202)	1.72	1.75
(522)	1.48	1.44
(571)	1.24	1.22
(652)	1.19	1.16
(453)	1.02	1.01
(173)	0.94	0.94
(014)	0.91	0.91
(624)	0.85	0.83
(824)	0.78	0.79

plasma plume can result in a lot of cases of collisions, then aggregations, and then condensations of the species. The phase transformation such as new molecule formation and nucleation could therefore take place in the plasma plume. In this case, the new nuclei, such as silver and nickel nuclei, will form in the plasma plume when the plasma plume's temperature and pressure start to drop down, due to mixing of silver, nickel, and oxygen atoms in the plasma plume. Subsequently, these nuclei diffuse randomly, and then aggregate when they encounter. Meanwhile, sufficient species and energy are available around the nuclei, because the plasma plume is confined in the silver nitrate solution. Thus, these nuclei will easily grow to be large. The trunks of the grown nanodendrites, consisting of silver nanoparticles in Figures 2 and 3, should form in the nucleation and growth process. Additionally, nickel nanoparticles also form in this stage. However, nickel clusters could go away from silver clusters when they encounter, due to the repulsive interaction between Ag and Ni atom [15]. The final stage is the plasma plume quenching process in liquid. The HPHT plasma plume will quench in the solution when the pulsed-laser is over. In the initial stage of the plasma plume quenching process, the solution at the interface between the plasma and liquid will continue to be decomposed and ionized into atoms and ions such as Ag and O, due to the HPHT situation of the plasma [20]. At the same time, owing to the cooling effect of the confinement liquid, the temperature gradient from the trunks

Table 2. Identification of the fcc phase silver grown upon pulsed-laser induced in silver nitrate solution. D_{exp} are the experimental data, and D_{calc} are the calculated values.

(*hkl*)	D_{exp} (Å)	D_{calc} (Å)
(111)	2.38	2.36
(200)	2.05	2.04
(220)	1.48	1.44
(311)	1.24	1.23
(222)	1.19	1.18
(400)	1.02	1.02
(331)	0.94	0.94
(024)	0.91	0.91
(224)	0.85	0.83
(333)	0.78	0.79

to liquid would be created in the nanoparticles, including the aggregating patterns in the HPHT state. Thus, when the temperature of the plasma plume quickly drops down, silver oxide would deposit on the surface of Ag nanoparticles in the direction of the temperature gradient from the nanoparticles to the liquid, and would display a radial shape, such as the nanoplumes shown in Figure 3. Silver oxides are unstable and are decomposed into silver and oxygen at high temperatures. Therefore, silver oxides cannot exist at the early stage after laser irradiation. Accordingly, the deposition of silver oxides should take place in the late stage of the plasma plume quenching process in the liquid. On the other hand, since the growth time (plasma quenching time) of nanostructures upon PLIIR is very short, the sizes of the grown crystals are usually on the nanometer scale [9], as in the experimental descriptions in our case. Moreover, the pulsed-laser power can greatly affect the structure and composition of the synthesized productions by PLIIR [13,14].

According to the discussions above, it is clear that the nanocomposites consisting of silver particles and silver oxide plumes grown upon PLIIR can not form during the natural drying process of the silver nitrate solution, since the strong interactions between the plasma plume and liquid (such as HPHT state, the temperature gradient, rapid quenching of the plasma plume, etc.) don't appear in the natural drying process. Therefore, the nanoparticles usually display sphere-like aggregations in the drying process due to the effect of the van der Waals force between nanoparticles.

4 Conclusions

In summary, we have shown the formation of an abnormal nanodendrite consisting of silver nanoparticles and silver oxide nanoplumes with polycrystalline structures upon PLIIR. Following our previous studies, a vapor-liquid mechanism was proposed for the growth of the synthesized nanopatterns, and both the silver clusters in vapor and the silver ions in solution are simultaneously

involved. This study and previous demonstrations from other groups [16–21] make it clear that PLIIR is an effective and general route for fabricating new nanostructures of metals, alloys, and inorganic compounds.

The authors are grateful for the support of the National Natural Science Foundation of the People's Republic of China (No. 50072022).

References

1. W.P. Helperin, Rev. Mod. Phys. **58**, 533 (1986)
2. A.C. Templeton, W.P. Wuelfing, R.W. Murray, Acc. Chem. Res. **33**, 27 (2000)
3. M.A. El-Sayed, Acc. Chem. Res. **34**, 257 (2001)
4. Y. Sun, Y. Xia, Science **298**, 2176 (2002)
5. H. Gleiter, Prog. Mater. Sci. **33**, 223 (1989)
6. L.K. Kurihara, G.M. Chow, P.E. Schoen, Nanostructure Mater. **5**, 605 (1995)
7. G.W. Yang, J.B. Wang, Q.X. Liu, J. Phys.: Condens. Matter **10**, 7923 (1998)
8. J.B. Wang, G.W. Yang, J. Phys.: Condens. Matter **11**, 7089 (1999)
9. J.B. Wang, C.Y. Zhang, X.L. Zhong, G.W. Yang, Chem. Phys. Lett. **361**, 86 (2002)
10. G.W. Yang, J.B. Wang, Appl. Phys. A **71**, 343 (2000)
11. C.Y. Zhang, X.L. Zhong, J.B. Wang, G.W. Yang, Chem. Phys. Lett. **370**, 522 (2003)
12. Q.X. Liu, G.W. Yang, J.X. Zhang, Chem. Phys. Lett. **373**, 56 (2003)
13. G.W. Yang, J.B. Wang, Appl. Phys. A **72**, 475 (2001)
14. Q.X. Liu, C.X. Wang, W. Zhang, G.W. Yang, Chem. Phys. Lett. **382**, 1 (2003)
15. G.W. Yang, W.S. Lai, C. Lin, B.X. Liu, Appl. Phys. Lett. **74**, 3305 (1999)
16. D. Poondi, J. Singh, J. Mater. Sci. **35**, 2467 (2000) and references therein
17. D. Poondi, T. Dobbins, J. Singh, J. Mater. Sci. **35**, 6237 (2000)
18. D.E. Wolfe, J. Singh, J. Senderson, J. Zabinski, J. Adv. Mater. **35**, 52 (2003)
19. Y.F. Lu, S.M. Huang, X.B. Wang, Z.X. Shen, Appl. Phys. A **66**, 543 (1998)
20. S. Zhu, Y.F. Lu, L.M. Hong, X.Y. Chen, J. Appl. Phys. **89**, 2400 (2000) and references therein
21. S. Zhu, Y.F. Lu, M.H. Hong Appl. Phys. Lett. **79**, 1396 (2001)